Inherent structures and distribution functions for liquids that freeze into bcc crystals

Thomas A. Weber and Frank H. Stillinger
AT&T Bell Laboratories, Murray Hill, New Jersey 07974

(Received 9 July 1984; accepted 2 August 1984)

The collection of potential energy minima in a condensed phase determines its inherent packing structures. We have examined these inherent structures for a simple model substance which (like Na) freezes into a bcc crystal. Molecular dynamics trajectories at several different temperatures were periodically sampled, and each of the configurations was "quenched" by a steepest-descent construction into a nearby potential energy minimum. The resulting collections of inherent structures possess quenched pair correlation functions that are nearly independent of the initial-state temperature, provided the latter correspond to fluid states. Attempts to reconstitute the equilibrium pair correlation functions by thermally broadening the quenched versions, using harmonic Einstein or Debye vibrational approximations, were clear failures. Evidently the true broadening phenomenon entails substantial anharmonicity.

I. INTRODUCTION

Understanding liquids remains a formidable challenge. Their structural diversity at the molecular level, the dependence of that diversity on interaction details, and how these features determine kinetics in liquids will doubtless remain active topics for at least the near future.

In order to simplify somewhat the theoretical problems posed by the liquid state we have introduced a viewpoint which formally separates geometric packing considerations from thermal excitations.[1–5] The molecular packings are defined to be local minima in the relevant potential energy function. By means of a steepest-descent connection on the multidimensional potential energy hypersurface any configuration of the molecules can uniquely be mapped onto a nearby potential minimum. Indeed we view this mapping simply as an operation for removing thermal excitation from any initial molecular configuration.

By definition the steepest-descent mapping permits no structural annealing to occur; potential energy barriers are never surmounted. In this sense it corresponds to an infinitely rapid quenching of the initial state, and for convenience we will refer below to the mapping as "quenching."

One of our earlier studies[6] focussed on the effect that steepest-descent quenching created in the pair correlation function $g^{(2)}$. The specific model investigated was that of a monatomic substance (such as the noble gases beyond helium) whose stable crystal form is face-centered cubic. Not surprisingly the constant-density quench procedure caused the pair correlation function $g^{(2)}(r)$ to change to a much more structured function $g_q^{(2)}(r)$. However, it *was* surprising to discover that at constant density the $g_q^{(2)}(r)$ was substantially independent of the temperature prevailing in the thermodynamically stable liquid before quenching. As a result it appeared that the liquid phase statistically possessed a temperature-independent inherent structure and that the temperature dependence of $g^{(2)}$ reflected only a variable extent of thermal excitation in the inherent packing structure.

The present project was undertaken in an effort to see if the previous observations had wider applicability. Specifically we have elected to examine another important class of monatomic models which, like many metallic elements such as Na, have the bcc crystal as their stable form at low temperature. The principal object has been to evaluate $g^{(2)}$ and $g_q^{(2)}$ for this new case and to see as before if the latter is substantially independent of the prequench temperature (at constant density).

Section II discusses the pair potential utilized, contrasting it with the previous case examined, and provides details of the classical molecular dynamics and numerical quenching procedures employed to study the liquid. Section III provides some results on the distribution in potential energy of the packing structures sampled in the liquid phase. Pair correlation functions before and after quench also appear in this section. Section IV establishes the importance of anharmonicity in the thermal excitation process that reconstitutes $g^{(2)}$ from $g_q^{(2)}$. The discussion contained in Sec. V anticipates several future applications.

The reader may wish to consult a companion paper[7] which discusses details of packing structures and their interconversions for the same model studied here.

II. MODEL SYSTEM

In a series of recent studies[4–8] we have chosen to use a pair potential of the form

$$\begin{aligned} v(r) &= A\,(r^{-p} - r^{-q})\exp[(r-a)^{-1}] \quad (0<r<a) \\ &= 0 \qquad\qquad\qquad\qquad\qquad\quad (a\leqslant r). \end{aligned} \tag{2.1}$$

The chief advantage of this potential is that $v(r)$ and all its derivatives go to zero at a. Previously the parameters A, p, q, and a were chosen so that the fcc lattice was the most stable 0 K crystal form. Therefore it was possible to simulate the noble gases such as argon.[4] Other choices of parameters will lead to other lattice structures being stabilized. In particular the choice

$$A = 3.809\,745\,436, \quad p = 6, \quad q = -1, \quad a = 2 \tag{2.2}$$

has the bcc lattice as the most stable crystal. Figure 1 shows a plot of the pair-interaction potential as a function of separa-

 0021-9606/84/235089-06$02.10

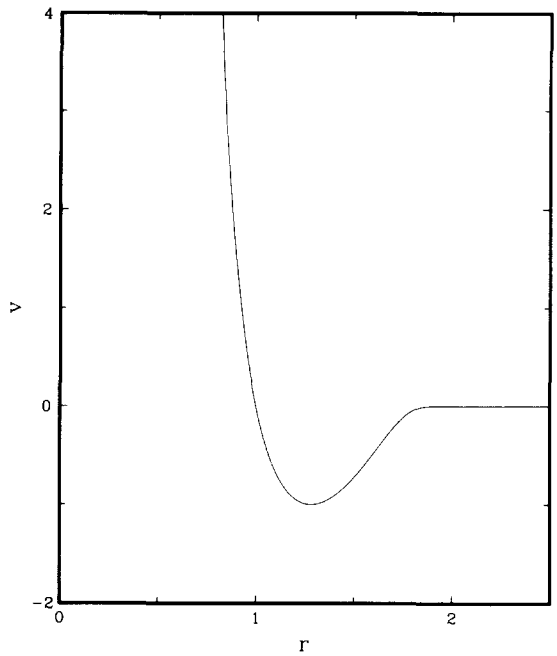

FIG. 1. Pair-interaction potential as a function of separation distance as given by Eqs. (2.1) and (2.2).

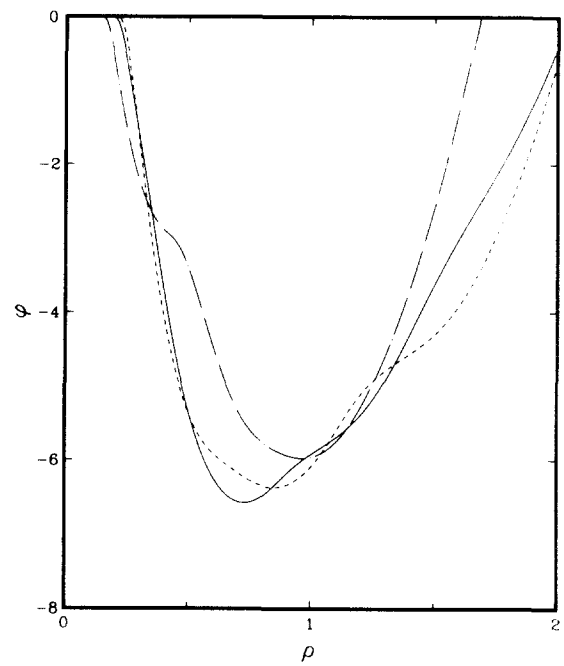

FIG. 2. Lattice energies per particle for the bcc (solid line), the fcc (dashed line), and simple cubic (dash-dot line) lattices.

tion distance for this choice of parameters. The minimum in v occurs at

$$r = 1.282\,283\,54 \tag{2.3}$$

and A has been chosen to yield a potential of -1 at the minimum. In order to represent a real substance this interaction potential will require that both the energy (ϵ) and length (σ) be rescaled:

$$\epsilon v(r/\sigma). \tag{2.4}$$

Values appropriate for Na, e.g., are

$$\epsilon = 1.191\,44 \times 10^{-14}\ \text{erg}, \quad \sigma = 0.289\,33\ \text{nm}, \tag{2.5}$$

to yield the observed lattice spacing and melting temperature. The fundamental time unit, taking the mass of one Na atom as 3.8193×10^{-23} g, is

$$\tau = \sigma(m/\epsilon)^{1/2} = 1.6384\ \text{ps}. \tag{2.6}$$

Figure 2 shows for v a plot of the energy per particle for the bcc, fcc, and simple cubic lattices as a function of density. The simulations described below were performed at reduced density

$$\rho^* = 0.730\,51 \tag{2.7}$$

corresponding to the minimum in the bcc curve in Fig. 2 which would be the zero pressure and zero temperature crystal structure. The absolute minimum in the total potential energy

$$\Phi = \sum_{i<j}^{N} v(r_{ij}) \tag{2.8}$$

for $N = 128$ particles corresponds to the perfect bcc lattice aligned with the sides of a cubical box; this has been our choice of system size and shape for molecular dynamics. The usual periodic boundary conditions have been applied so as to simulate the bulk phase. The potential energy per particle at the absolute minimum is

$$\phi = \Phi/N = -6.578\,015. \tag{2.9}$$

Notice that for our previous simulation of the fcc system that $\phi = -6.000\,00$ indicative of the fact that only nearest neighbor interactions were important, whereas with this potential (2.2) the contributions from second neighbor interactions are substantial. It should also be noted that as the density is increased there will be a transition from bcc to fcc and then from fcc to sc. Eventually the fcc structure will dominate at the highest densities.

Molecular dynamics runs were created at various temperatures in both the fluid and crystalline (frozen) states. The details of the melting and freezing processes will be reported in a companion paper.[8]

The Newtonian equations of motion were integrated using a fifth-order Gear algorithm[9] with a time step in reduced units of

$$\Delta t = 0.001\,25. \tag{2.10}$$

Each run was first equilibrated for at least 2×10^3 time steps and runs were typically 10^4 time steps long (20.48 ps for Na). No momentum scaling was necessary because the total energy was conserved to high accuracy during the run. While the trajectory was being generated, usually the configurations at every $100\Delta t$ were quenched to locate the nearest Φ-minimum packing structure. The trajectory configurations themselves were left undisturbed, serving only as initial conditions for locating the minima. The quenching procedure, which has been previously described,[5] was used to find the stable packing configurations of the system by solving

$$\nabla\Phi(r) = 0. \tag{2.11}$$

A combination of a Newton's method and a conjugate-gradient method[10] was used to produce the relevant solutions of Eq. (2.11).

The simulations were initiated from the perfect bcc

crystal by slow heating. The crystal was melted and the temperature raised stepwise to $T^* = 1.9$. The fluid was then cooled in stages and allowed to recrystallize. The melting and freezing curves were traversed several times. Using this procedure at our fixed density we estimate the melting temperature to be

$$T_m^* \approx 0.43 \tag{2.12}$$

in reduced units.

III. QUENCH ENERGY AND STRUCTURE

In our previous studies of argon[5] it was shown that the rate at which particles undergo transitions between regions of different packing structures is a strong function of both the density and the temperature of the system. Figure 3 shows a plot of the quench energy per particle for a 140 step run which was quenched every time step. The system, in a slightly supercooled liquid state, had an average temperature $T^* = 0.40$ which was close to the melting point ($T_m^* \approx 0.43$). There were 65 transitions between the packings that were observed and a total of 39 different packings were sampled. The absolute minimum energy configuration however was not observed although configurations in two low lying bands were observed. These bands are due to the single and double vacancy/split-interstitial pair defects which are discussed in greater detail in the companion paper.[7] The majority of quench structures observed are amorphous packings of much higher energy.

Figure 4 shows a plot of quench energy for a liquid sample at $T^* = 0.41$ which was run 10^4 time steps. The quenching procedure was performed every 100 steps. Many transitions have undoubtedly occurred between successive sample quenches. Notice also that the absolute-minimum-energy packing structure has been observed twice in this run. A similar plot is shown in Fig. 5 where the trajectory average temperature was $T^* = 1.90$. The chief difference between Figs. 4 and 5 is that the low-energy inherent structures are encountered more frequently at the lower temperature.

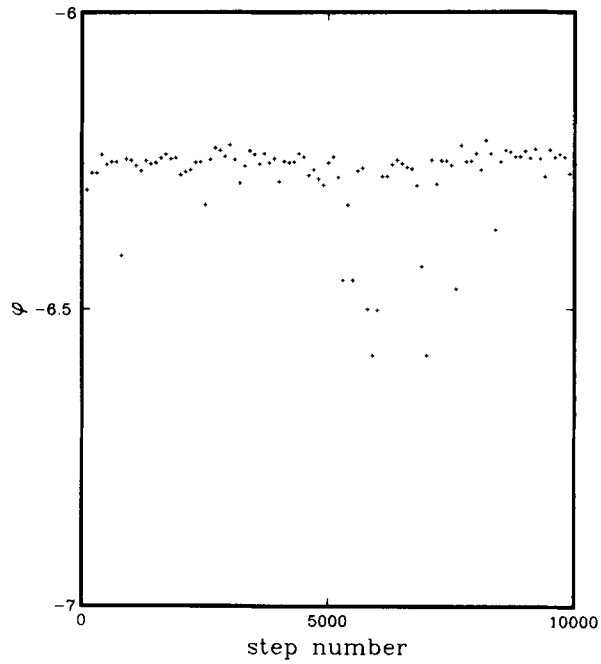

FIG. 4. Sequence of local minima for a run whose prequench reduced temperature was 0.41. The system was quenched 101 times during the 10^4 time step run.

Figures 6 and 7 show the liquid-state pair correlation function $g^{(2)}(r)$ for the two temperatures 0.41 and 1.90, respectively. The small system size (periodic box length is 5.596 in reduced units) makes it impossible to measure $g^{(2)}(r)$ past reduced distance 2.75 because of the intrusion of the

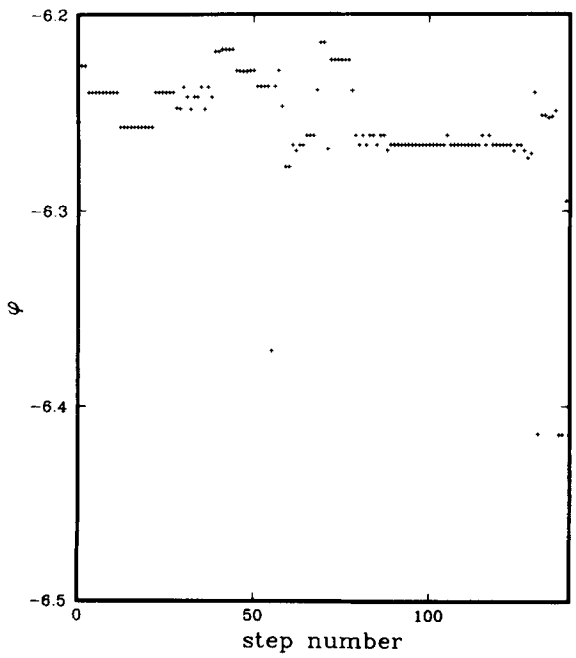

FIG. 3. Sequence of local minima in the potential (on a per particle basis) resulting from steepest-descent mapping. The initial reduced temperature was 0.396. The quenching was performed every step of this 140 time step run.

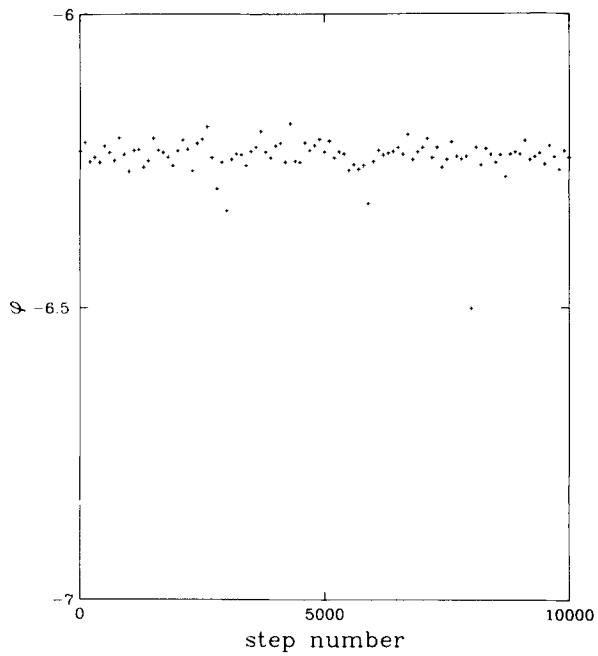

FIG. 5. Sequence of local minima for a run whose prequench reduced temperature was 1.90.

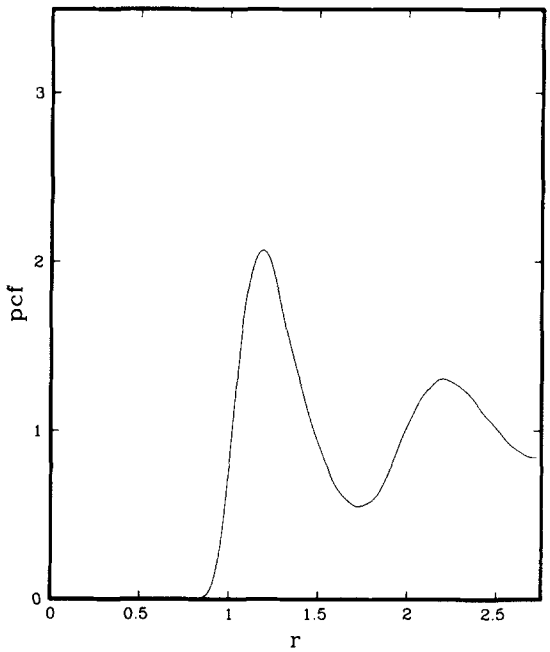

FIG. 6. Pair correlation function for the bcc fluid with prequench reduced temperature of 0.41.

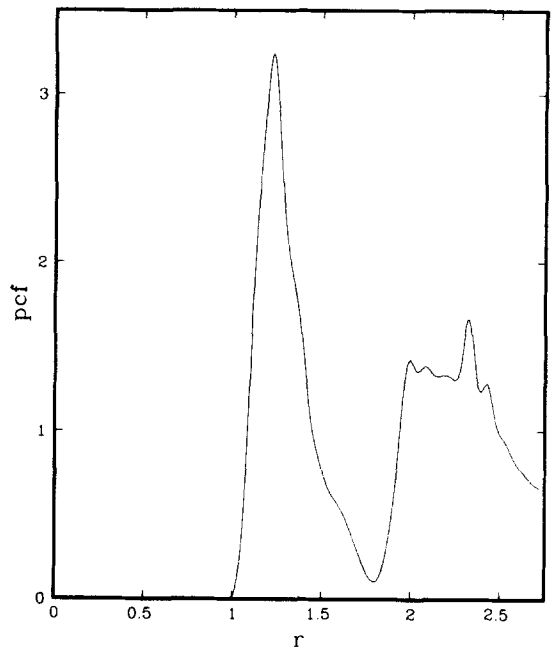

FIG. 8. Pair correlation constructed from the 101 quench configurations generated from the trajectory whose prequench reduced temperature was 0.41.

periodic image. However a well resolved first and second peak are observed. The amplitude of the first peak clearly decreases with increasing temperature, as expected, due to thermal broadening.

Pair correlation functions have been constructed from the 101 quench configurations which were generated during the two preceding long trajectory calculations. Figures 8 and 9 present pair correlation functions $g_q^{(2)}(r)$ for the prequench temperatures $T^* = 0.41$ and $T^* = 1.90$, respectively. Contrasting Figs. 6 and 7 with Figs. 8 and 9 respectively shows the great extent to which the quenching procedure has enhanced the structure of the pair correlation functions.

Examination of the $g_q^{(2)}(r)$ in Figs. 8 and 9 for the two prequench temperatures shows that in both curves the first peaks are nearly identical and that the broad based second peak from 2 to 2.5 overall is also nearly the same. The differences between the two reside in the height of the little peaks on the underlying broadened second peak. These small and narrow peaks are attributable to the perfect (or nearly perfect) crystalline configuration. Thus their amplitudes depend strongly on the number of times the minimum energy

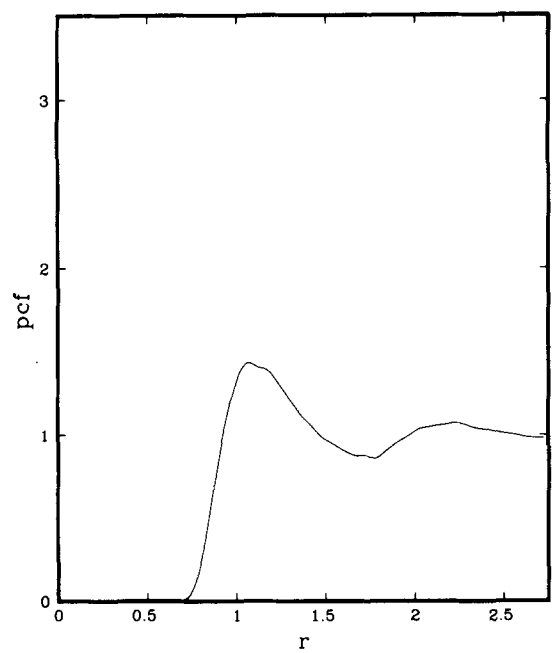

FIG. 7. Pair correlation function for the bcc fluid with prequench reduced temperature of 1.90.

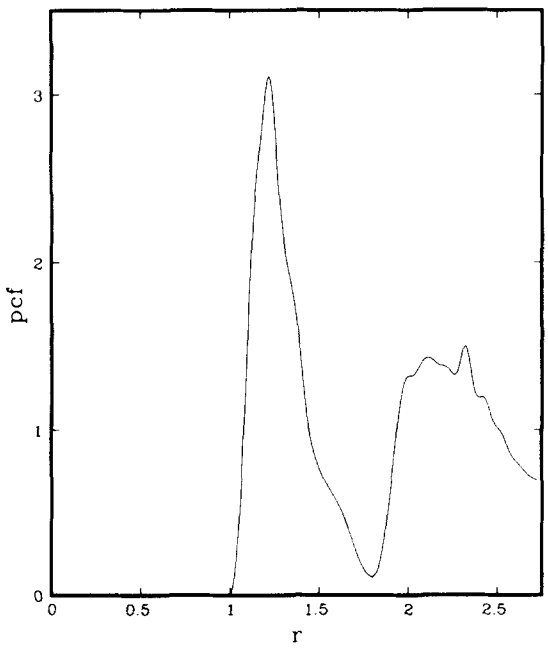

FIG. 9. Pair correlation constructed from the 101 quench configurations generated from the trajectory whose prequench reduced temperature was 1.90.

configuration and the configurations in the two low lying bands due to vacancy/split-interstitial pair defects are sampled. It is worth noting that these peaks are subject to large statistical uncertainty since only a very small number $\leqslant 10\%$ of these states are found at any given prequench temperature in the fluid. Our other quenching results for this model bear out that premise and suggest that suitable extended averaging over quench structures would indeed yield a temperature-independent $g_q^{(2)}(r)$ intermediate between those in Figs. 8 and 9.

IV. THERMAL BROADENING

Since the removal of vibrational motion produces pair correlation functions which are nearly temperature independent it is tempting to try to reverse this process, i.e. to thermally broaden the quench pair correlation functions $g_q^{(2)}(r)$ to produce the temperature dependent pair correlation functions $g^{(2)}(r,\beta)$. The simplest way to attempt this broadening is to use an Einstein approximation. A slightly more sophisticated approach which incorporates both longitudinal and transverse phonon modes is the Debye approximation. A simple generic formula which may be used to accomplish this broadening using either the Einstein or Debye approximations is

$$g^{(2)}(R,\beta) = \frac{1}{\pi^{1/2}R}\int_0^\infty dr\, r\, g_q^{(2)}(r)[\beta\alpha(r)]^{1/2} \times\{\exp[-\beta\alpha(r)(R-r)^2] - \exp[-\beta\alpha(r)(R+r)^2]\}, \quad (4.1)$$

where $\beta = 1/k_B T$, $g_q^{(2)}(r)$ is the quench pair correlation function as before, and $\alpha(r)$ is a broadening function. The Einstein model takes $\alpha(r)$ as a constant. In the Debye approximation $1/\alpha(r)$ is a constant at large r and starts off at least quadratically at small r.

A generic broadening function of the form

$$1/\alpha(r) = Ar^{2j}/(1 + Br^{2j}) \quad (4.2)$$

has been used to attempt to reproduce the observed thermal broadening behavior of $g^{(2)}(r,\beta)$. The temperature-independent pair correlation function $g_q^{(2)}(r)$ as determined from the simulations was used in Eq. (4.1) and the parameters A, B, and j (= 1, 2, or 3) were chosen to give the best possible fit to the pair correlation function $g^{(2)}(r)$ at a given temperature. The criterion used for best fit was to pick the parameters so as most closely to match the height and position of the first peak in $g^{(2)}$ and also to minimize the discrepancy between the predicted and calculated values of the first valley and second peak of the pair correlation function. This optimal choice of A, B, and j was then used to predict the thermally broadened pair correlation function at the other temperature.

It was not possible to obtain good fits between the predicted and calculated pair correlation functions by simply adjusting the parameters of Eqs. (4.1) and (4.2). In addition, whether the parameters were chosen from the best fit to the high temperature pair correlation function ($T^* = 1.90$) or to the low temperature pair correlation function ($T^* = 0.41$) the predictions at the other temperature were unsatisfactory. Furthermore no reasonable extension of form (4.2) rectifies matters.

In each case the predicted pair correlation function $g^{(2)}(r,\beta)$ was more correlated than was observed from the simulations. This difficulty may stem from the quadratic approximation used in the exponentials of Eq. (4.1). At present simple attempts to thermally broaden the temperature independent pair correlation functions do not produce the observed $g^{(2)}(r,\beta)$.

V. DISCUSSION

The procedure of quenching trajectory configurations to reveal the underlying packing structures has again proven to be useful. As was the case with the "fcc" fluid,[6] a temperature-independent pair correlation function was discovered for the bcc potential. For that prior case it was possible to relate the quench pair correlation function to that of a structurally disordered perfect crystal. No such simple explanation is at first glance possible for the bcc system probably due to the fact that the bcc potential is much softer than its fcc counterpart and therefore permits a larger density of defects in the packing structures underlying its liquid phase.

The running coordination number $n(r)$ is defined by the equation

$$n(r) = 4\pi\rho^* \int_0^r s^2 g^{(2)}(s)\, ds. \quad (5.1)$$

It is common practice to define the number of nearest neighbors in simple atomic fluids as $n(r_1)$, where r_1 is the position of the first minimum in the pair correlation function. Using this convention the number of nearest neighbors is found to be 15.0 and 16.3 for $T^* = 0.41$ and $T^* = 1.90$, respectively. If instead the number of nearest neighbors is determined from the quench pair correlation function, then $n_q(r_1)$ is found to be 15.4 for both temperatures. Thus once thermal motion is removed the number of nearest neighbors in the fluid is nearly temperature independent. This suggests that structural interpretations of liquids based solely on their $g^{(2)}$'s can be somewhat misleading.

It was not possible to reconstitute the temperature dependence of the pair correlation functions by thermally broadening the temperature-independent quench pair correlation function $g_q^{(2)}(r)$. Since both the Einstein and Debye approximations rely on a Gaussian convolution to thermally broaden the pair correlation functions, the lack of success is a strong indication of the importance of local anharmonic effects. It may be necessary to replace the functional form of Eq. (4.1) with a more general functional form to meet with success. Possibly replacing $\exp[-\alpha(r)(R \pm r)^2]$ with $\exp[-\alpha(r)(R \pm r)^p]$ would account for the anharmonicity and represent a simple way to introduce thermal broadening. However we feel that a purely empirical search of this kind would be inappropriate at this stage.

That both the fcc and "bcc" fluids possess temperature-independent quench radial distribution functions lends further credence to our approach of separating the partition function into a part related to the packing structures and a vibrational component. This approach is quite general and has been successfully applied to more complex systems such as the binary alloy $Ni_{80}P_{20}$.[11] As long as the prequench temperature is sufficiently high so that any trajectory can effec-

tively sample the entire phase space, the quench pair correlation functions show little temperature dependence, quite independently of interaction details.

[1]F. H. Stillinger and T. A. Weber, Kinam **3A**, 159 (1981).
[2]F. H. Stillinger and T. A. Weber, Phys. Rev. A **25**, 978 (1982).
[3]F. H. Stillinger and T. A. Weber, J. Phys. Chem. **87**, 2833 (1983).
[4]F. H. Stillinger and T. A. Weber, Phys. Rev. A **28**, 2408 (1983).
[5]T. A. Weber and F. H. Stillinger, J. Chem. Phys. **80**, 2742 (1984).
[6]F. H. Stillinger and T. A. Weber, J. Chem. Phys. **80**, 4434 (1984).
[7]F. H. Stillinger and T. A. Weber, J. Chem. Phys. **81**, 5095 (1984).
[8]F. H. Stillinger and T. A. Weber, (to be published).
[9]C. W. Gear, Argonne National Lab. Report ANL-7126, January, 1966.
[10]R. Fletcher, *Practical Methods of Optimization* (Wiley, New York, 1980).
[11]F. H. Stillinger and T. A. Weber, Science **225**, 983 (1984).